JOURNAL OF VIROLOGY, Aug. 2005, p. 9991–10002 Vol. 79, No. 15
0022-538X/05/$08.00+0 doi:10.1128/JVI.79.15.9991–10002.2005

Molecular Basis for Mitochondrial Localization of Viral Particles during *Beet Necrotic Yellow Vein Virus* Infection

Clarisse Valentin, Patrice Dunoyer, Guillaume Vetter,† Catherine Schalk,‡ André Dietrich,* and Salah Bouzoubaa

Institut de Biologie Moléculaire des Plantes du CNRS, Université Louis Pasteur, 12 rue du Général Zimmer, 67084 Strasbourg, France

Received 29 December 2004/Accepted 16 April 2005

During infection, *Beet necrotic yellow vein virus* (BNYVV) particles localize transiently to the cytosolic surfaces of mitochondria. To understand the molecular basis and significance of this localization, we analyzed the targeting and membrane insertion properties of the viral proteins. ORF1 of BNYVV RNA-2 encodes the 21-kDa major coat protein, while ORF2 codes for a 75-kDa minor coat protein (P75) by readthrough of the ORF1 stop codon. Bioinformatic analysis highlighted a putative mitochondrial targeting sequence (MTS) as well as a major (TM1) and two minor (TM3 and TM4) transmembrane regions in the N-terminal part of the P75 readthrough domain. Deletion and gain-of-function analyses based on the localization of green fluorescent protein (GFP) fusions showed that the MTS was able to direct a reporter protein to mitochondria but that the protein was not persistently anchored to the organelles. GFP fused either to MTS and TM1 or to MTS and TM3-TM4 efficiently and specifically associated with mitochondria in vivo. The actual role of the individual domains in the interaction with the mitochondria seemed to be determined by the folding of P75. Anchoring assays to the outer membranes of isolated mitochondria, together with in vivo data, suggest that the TM3-TM4 domain is the membrane anchor in the context of full-length P75. All of the domains involved in mitochondrial targeting and anchoring were also indispensable for encapsidation, suggesting that the assembly of BNYVV particles occurs on mitochondria. Further data show that virions are subsequently released from mitochondria and accumulate in the cytosol.

Viruses recruit a variety of structures and pathways in infected host cells to develop their life cycle. These processes are critical for the development of infection and are mediated by viral-encoded polypeptides. Characterizing the subcellular localization of viral proteins and establishing a relationship between localization and activity are therefore of fundamental relevance. Many viruses, especially eukaryotic positive-sense single-stranded RNA viruses, transiently interact with cellular membranes. Depending on the virus, a variety of membrane systems can be targeted (7). Among these, mitochondria can play an important role and have received increasing interest during the last few years in view of their role in apoptosis. The previously described interactions between viruses and mitochondria involve anchoring of the replication complex to the organelle outer membrane (20, 34, 55) or molecular processes which might be related to host cell death (3, 18, 51). Like regular organelle proteins, viral proteins that associate with mitochondria typically carry transmembrane domains and mitochondrial targeting signals. This is the case for protein A of betanodaviruses (20), for the RNA polymerase of *Flock house virus* (34), and for the core protein of *Hepatitis C virus* (51). Concerning plant viruses, it has recently been reported that *Carnation Italian ringspot virus*, a *Tombusvirus*, encodes a transmembrane domain-containing replicase that localizes to mitochondria and is anchored to the mitochondrial outer membrane by an import receptor-independent signal-anchor mechanism (55).

The mitochondrial localization of virions has been observed with *Rubella virus* (RV) (3) and in early electron microscopy studies with *Tobacco rattle virus* (22, 23). Organelle targeting of RV nucleocapsids is probably mediated by an interaction between the capsid protein and a host mitochondrial protein (3). No further data are available about the mitochondrial localization of *Tobacco rattle virus* particles. We have previously shown that *Beet necrotic yellow vein virus* (BNYVV) particles localize to the cytosolic surfaces of mitochondria in *Chenopodium quinoa* leaves at an early stage of infection (15). This process was not related to replication, as immunolabeling analyses (13) indicated that BNYVV RNA replication occurs in the cytosol and does not involve mitochondrial membranes (Mathieu Erhardt, unpublished results). Thus, a study of the association of BNYVV particles with mitochondria may reveal novel aspects of the biology of this virus.

BNYVV, the type species of the genus *Benyvirus*, is a multipartite, positive-strand RNA virus transmitted by a soilborne fungus, *Polymyxa betae*. Depending on the isolate, the BNYVV genomic information is carried by four or five RNA molecules which are capped at the 5′ end and polyadenylated at the 3′ end (42, 47, 52). Although all RNAs are indispensable for the natural infection of plants in the field, RNA-1 and -2 alone are sufficient for the infection cycle in leaves and in protoplasts of

* Corresponding author. Mailing address: Institut de Biologie Moléculaire des Plantes du CNRS, 12 rue du Général Zimmer, 67084 Strasbourg, France. Phone: 33 3 88 41 72 41. Fax: 33 3 88 61 44 42. E-mail: andre.dietrich@ibmp-ulp.u-strasbg.fr.

† Present address: CRP-Santé, Laboratory of Molecular Biology, Functional Genomics and Modeling (LBMAGM), 42 rue du Laboratoire, L-1011 Luxembourg, Luxembourg.

‡ Present address: TEPRAL, Centre de Recherche des Brasseries Kronenbourg, 68 route d'Oberhausbergen, 67000 Strasbourg, France.

C. quinoa (6) or *Nicotiana tabacum* BY2 (35). RNA-1 carries the information for replication (5), while RNA-2 carries information involved in viral assembly and transmission by the fungal vector (major and minor coat proteins [50, 53]) (Fig. 1A), in cell-to-cell movement of the virus (proteins encoded by the "triple gene block" [19]), and in suppression of posttranscriptional gene silencing (P14 [12, 24]).

The BNYVV particle consists of a molecule of viral RNA packaged into a nucleoprotein helix by association with multiple copies of the major coat protein (CP). One or a few copies of a minor coat protein (P75) produced by translational readthrough of the CP stop codon are attached to an extremity of the virion (21). The readthrough domain (RTD) of P75 probably protrudes from the particles, as it is accessible to immunolabeling. In the present work, we present evidence implicating P75 in the anchoring of BNYVV virions to the mitochondria. A bioinformatic sequence analysis of P75 highlighted a putative mitochondrial targeting sequence and several candidate transmembrane domains in the N-terminal part of the RTD. These sequences were used for deletion and gain-of-function studies. To this end, different enhanced green fluorescent protein (GFP) fusions were expressed in vivo, and their subcellular localization was observed by laser scanning confocal microscopy. The predicted organelle targeting sequence directed highly efficient and specific binding to mitochondria, but a stable mitochondrial association required the presence of a transmembrane domain. Deletion of the targeting sequence abolished not only mitochondrial targeting but also viral assembly. In vitro membrane insertion assays in the presence of isolated plant mitochondria demonstrated that P75 associates with the organelles as an integral protein in the outer membrane, with both the N terminus and the C terminus exposed to the cytosol. The results are discussed in view of their significance in BNYVV biogenesis and in the light of known mechanisms of targeting and integration of proteins into the mitochondrial outer membrane.

MATERIALS AND METHODS

Computer analysis of BNYVV sequences. A computer search for putative mitochondrial targeting sequences was carried out with the following three prediction programs, taking into account plant presequences: Predotar (http://genoplante-info.infobiogen.fr/predotar/predotar.html), Psort (http://psort.nibb.ac.jp/; 36), and TargetP (http://www.cbs.dtu.dk/services/TargetP/; 14). The following three programs were used to predict transmembrane domains: Argos transmembrane (39), TMPRED (http://www.ch.embnet.org/software/TMPRED_form.html; 27), and von Heijne transmembrane (http://www.sbc.su.se/~miklos/DAS/; 10).

Construction of recombinant plasmids. All constructs were routinely sequenced to avoid unwanted modifications. Constructs pB2-RT-GFP1 and pB2-RT-GFP2 (Fig. 1B) have been described previously (15). They were both derived from pB2-14 (4, 53), which contains the wild-type BNYVV RNA-2 cDNA (Fig. 1A) cloned into pBluescribe (Clontech). Construct pB2-RT-GFP3 (Fig. 1B) was prepared following a similar strategy. The GFP sequence (46) without a stop codon was amplified by PCR with an AccI site at both ends and then cloned in frame into the $AccI_{1415}$ site of the BNYVV RNA-2 cDNA using a partial AccI digest of pB2-14 to keep the $AccI_{1415}$-$AccI_{1828}$ sequence in the construct. To generate the deletion mutant pB2-RT-Δ50-GFP2 (Fig. 1C), the $NcoI_{668}$-$MluI_{1139}$ fragment in pB2-RT-GFP2 was replaced by the corresponding fragment excised from the previously described mutant RNA-2 plasmid pB2-14-Δ50, which carries a deletion of nucleotides 793 to 894 (53).

For gain-of-function assays, DNA fragments spanning nucleotides 712 to 882, 712 to 960, 712 to 1053, 883 to 1053, 961 to 1053, and 1054 to 1335 of BNYVV RNA-2 (encoding amino acids 190 to 246, 190 to 272, 190 to 303, 247 to 303, 273 to 303, and 304 to 397 of the P75 protein) were amplified by PCRs using the plasmid pB2-UAU (50) (Fig. 1F), containing the complete P75 cDNA, as a template. In the direct primers p712S (5′-ATA*GGATCC*ATGCAATTAGCTGCTGCTCG-3′), p883S (5′-ATA*GGATCC*ATGGATATTGGCGGTCTTGTTAC-3′), p961S (5′-ATA*GGATCC*ATGGCAAATAGAAATAGCCTATG-3′), and p1054S (5′-ATA*GGATCC*ATGCAAAGTAGATTACGTGAG-3′), the BNYVV-specific sequences were complemented with a methionine-encoding ATG codon (underlined) and a BamHI site (italics) at the 5′ end. The reverse primers p882AS (5′-ATA*CCCGGG*ATCAGCAGCCAATTTGGC-3′), p960AS (5′-ATA*CCCGGG*CTGCTCAACTTCCTCAG-3′), p1053AS (5′-ATA*CCCGGG*GAGCTTCTTCCTATGATAAG-3′), and p1335AS (5′-ATA*CCCGGG*TCTAACAGTGTAAAATAAATC-3′) had an XmaI site (italics) at the 5′ end. The six PCR-amplified products were digested with BamHI and XmaI and inserted into the plasmid pRep-GFP (16) linearized with the same restriction enzymes, yielding constructs pRep-MTS-GFP, pRep-MTS-IS-GFP, pRep-MTS-IS-TM1-GFP, pRep-IS-TM1-GFP, pRep-TM1-GFP, and pRep-TM3-TM4-GFP (Fig. 1D). The DNA fragment spanning nucleotides 1054 to 1335 of BNYVV RNA-2 and encoding amino acids 304 to 397 of P75 was also amplified with a direct primer (p1054XmaS [5′-ATA*CCCGGG*CAAAGTAGATTACGTGAG-3′]) possessing an XmaI site (italics) at the 5′ end, whereas p1335AS was kept as the reverse primer. The resulting PCR product was digested with XmaI and inserted into pRep-MTS-IS-GFP linearized with the same restriction enzyme, yielding construct pRep-MTS-IS-TM3-TM4-GFP (Fig. 1D). The pRep plasmids are replicons derived from the BNYVV RNA-3 cDNA. They retain the RNA-3 noncoding sequences required for recognition by the BNYVV replicase/RNA-dependent RNA polymerase (nucleotides 1 to 382 and 1472 to 1774) and allow the in vivo expression of recombinant sequences (inserted between the two RNA-3 domains) when coinfected with RNA-1 alone or with RNA-1 and RNA-2 (29). The pRep plasmids also contain the phage T7 RNA polymerase promoter and thus were used as templates for in vitro synthesis of the recombinant RNAs to be electroporated.

For transient expression, DNA fragments corresponding to nucleotides 712 to 1053 and 883 to 1053 of BNYVV RNA-2 (encoding amino acids 190 to 303 and 247 to 303 of the P75 protein), already fused to the GFP gene, were amplified by PCRs using the plasmid pRep-MTS-IS-TM1-GFP as a template. The direct primers NcoMTS (5′-ATA*CCATGG*CACAATTAGCTGCTGCTCGGGTGACGGCACAC-3′) and NcoISTM1 (5′-ATA*CCATGG*ATATTGGCGGTCTTGTTAC-3′) contained an NcoI site (italics) providing the BNYVV-specific sequences with a 5′ in-frame methionine-encoding ATG codon (underlined). The reverse primer BamGFP (5′-ATA*GGATCC*TTACTTGTACAGCTCGTCC-3′) was complementary to the 3′ end of the GFP gene and contained a BamHI site (italics) at the 5′ end. The PCR-amplified fragments were digested with NcoI and BamHI and inserted into the pΩ plasmid (41) linearized with the same restriction enzymes, yielding pΩ-MTS-IS-TM1-GFP and pΩ-IS-TM1-GFP (Fig. 1E). The pΩ vector is designed for the in vivo transient expression of recombinant sequences under control of the *Cauliflower mosaic virus* 35S constitutive promoter and terminator. Translation is enhanced by the Ω leader of *Tobacco mosaic virus* (17). To construct the pΩ-GFP plasmid (Fig. 1E), the GFP gene was amplified as a 5′ NcoI/3′ BamHI PCR fragment and inserted into the pΩ plasmid (41) linearized with the same restriction enzymes.

Constructs pB2-UAU and pB2-TS (Fig. 1F), used for in vitro transcription/translation of the BNYVV major and minor coat proteins, were prepared in earlier studies (50). To generate the deletion mutant pB2-UAU-ΔTM1 (Fig. 1F), an $NcoI_{668}$-$MluI_{1139}$ fragment deprived of nucleotides 961 to 1053 was amplified by PCR using a reverse megaprimer (5′-AGC*ACGCGT*GTGCAGCTCAGTGCCGAAACCACCACCACCAGACCCACCAGTAGAGCCCCATAGTAATTTTAACTCACGTAATCTACTTTGCTGCTCAACTTCCTCAGAAAC-3′; the MluI site is in italics) and a couple of regular primers (5′-TTA*CCATGG*ACACCTGTTC-3′ [the NcoI site is in italics] and 5′-AGC*ACGCGT*GTGCAGCTC-3′ [the MluI site is in italics]). The PCR product obtained was exchanged for the $NcoI_{668}$-$MluI_{1139}$ fragment in pB2-UAU.

In vitro transcription and inoculation of protoplasts. Capped in vitro transcripts were obtained from the above-mentioned constructs with a T7 Ribomax transcription kit (Promega) following the manufacturer's instructions. Full-length wild-type BNYVV RNA-1 was synthesized from pB15 (43). pB2-14 and pB2-14-derived plasmids were linearized with SalI, whereas pB15, pRep, and pRep-derived plasmids were linearized with HindIII before transcription.

Protoplasts from *N. tabacum* BY2 cells (35) were prepared as previously described (26). The inoculation of protoplasts (10^6 in 0.5 ml) was done by electroporation (11) with 5 μg of transcript derived from the pB2- or pRep-derived constructs, together with 10 μg of RNA-1 transcript or 10 μg of RNA-1 and 5 μg of RNA-2 transcript. Electroporation was carried out at 125 μF, 180 V, and 100 Ω. For transient expression, BY2 protoplasts were electroporated with 25 μg of the corresponding pΩ plasmid at 125 μF, 280 V, and 100 Ω.

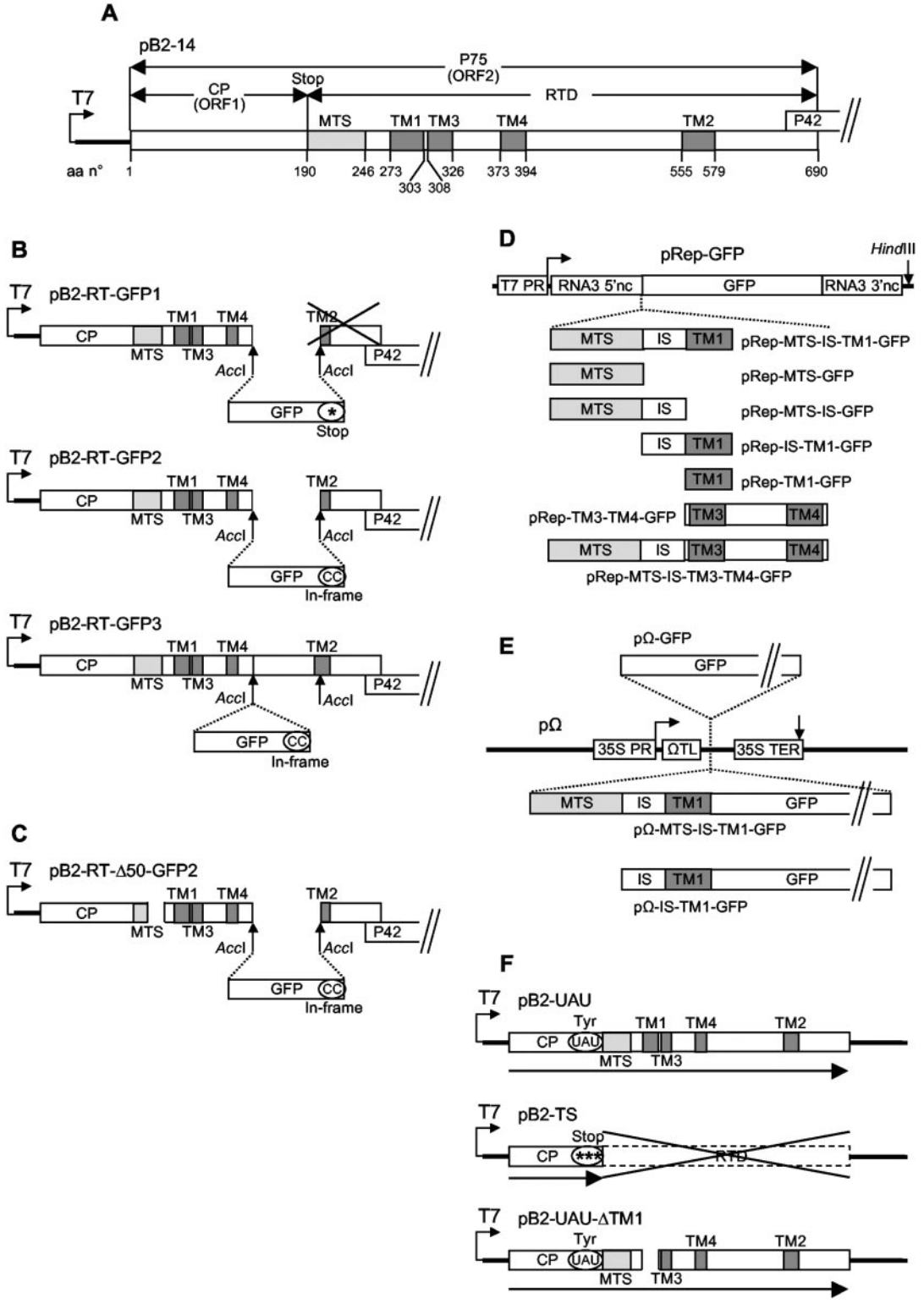

FIG. 1. Organization of the gene constructs used for the present study. (A) Plasmid pB2-14 contains the complete cDNA for BNYVV RNA-2 in pBluescribe (4, 53). Only ORF1 and ORF2 are represented. Amino acid (aa) numbers are indicated. (B) In plasmids pB2-RT-GFP1 and pB2-RT-GFP2 (15), the GFP gene replaces the $AccI_{1415}$-$AccI_{1828}$ sequence of pB2-14, truncating the TM2 domain; in pB2-RT-GFP3, the GFP gene is inserted in frame into the $AccI_{1415}$ site of pB2-14. (C) pB2-RT-Δ50-GFP2 derives from pB2-RT-GFP2 and carries a deletion of nucleotides 793 to 894, truncating the MTS domain. (D) The MTS, IS, TM1, and TM3-TM4 domains, individually or in combination, were inserted in frame with the GFP gene between the upstream and downstream noncoding sequences of the cDNA for BNYVV RNA-3 in the pRep replicon (16). (E) The GFP gene alone or the MTS-IS-TM1 or IS-TM1 domain fused to the GFP gene was inserted into the expression cassette of the pΩ plasmid (41). (F) In pB2-UAU, the CP sequence ends with a tyrosine codon, allowing full readthrough, whereas in pB2-TS the CP sequence ends with three stop codons, preventing readthrough; pB2-UAU-ΔTM1 carries a deletion of nucleotides 961 to 1053, eliminating the TM1 domain. *, stop codons; "(CC)" indicates that two extra C residues were added at the end of the GFP sequence to ensure the in-frame insertion; UAU, the stop codon of ORF1 was mutated to a UAU tyrosine codon. For more details, see Materials and Methods.

Laser scanning confocal microscopy. Observations of protoplasts pretreated with the mitochondrion-specific dye MitoTracker (CMTMRos; Molecular Probes) were carried out with a Zeiss LSM-510 confocal microscope. For GFP imaging, excitation at 488 nm was obtained with an argon laser, and for MitoTracker, excitation at 543 nm was obtained with a helium-neon laser. Appropriate emission filters were used to collect the green and red signals simultaneously from the same optical section without an overspill of fluorescence.

In vitro protein synthesis and membrane insertion tests with isolated plant mitochondria. A Promega TNT coupled transcription-translation kit was used for the in vitro synthesis of [^{35}S]methionine- or [^{3}H]leucine-labeled polypeptides according to the manufacturer's instructions. The pB2-UAU, pB2-TS, and pB2-UAU-ΔTM1 plasmids (Fig. 1F) were used as templates. Mitochondria were isolated from potato (*Solanum tuberosum*) tubers as described previously (30, 37). Membrane insertion tests with in vitro-synthesized viral polypeptides and fusion proteins were performed using mitochondrial protein import procedures essentially according to the work of Wischmann and Schuster (56). To characterize membrane-protected regions, incubation of the mitochondria with the labeled polypeptides was followed by a treatment with proteinase K (100 μg/ml) for 5 min at room temperature and 10 min on ice. Mitochondria were subsequently centrifuged through a 27% (wt/vol) sucrose cushion in 10 mM HEPES-KOH, pH 7.5. To test the membrane integration of the different BNYVV polypeptides, the mitochondrial samples were resuspended in 0.1 M Na_2CO_3 (pH 11.5)–1 mM phenylmethylsulfonyl fluoride, incubated for 30 min on ice, and centrifuged at 230,000 × *g* for 20 min, yielding a membrane pellet which retained integral proteins and a supernatant which contained proteins released from the membranes. Samples were analyzed by sodium dodecyl sulfate-polyacrylamide gel electrophoresis (31).

RESULTS

Identification of a candidate sequence for mitochondrial targeting. The major and minor coat proteins appeared as obvious candidates for mediating the mitochondrial localization of whole BNYVV particles. The 21-kDa major coat protein (CP; 188 amino acids) is encoded by ORF1 in BNYVV RNA-2. Readthrough of the stop codon of ORF1 allows the expression of ORF2 (Fig. 1A). The latter codes for the 75-kDa minor coat protein (P75), which is composed of the major coat protein (CP; amino acids 1 to 188) and a 54-kDa C-terminal readthrough domain (RTD; amino acids 189 to 690). No expression of this 54-kDa open reading frame by a mechanism other than readthrough has been detected (38). In the earlier experiments of Erhardt et al. (15), the replacement of amino acids 424 to 690 of the P75 protein by GFP (construct pB2-RT-GFP1) (Fig. 1B) to generate fluorescent virions did not abolish the mitochondrial localization of the viral particles in BNYVV RNA-infected *C. quinoa* leaves or *N. tabacum* protoplasts. This domain thus seemed to be dispensable for specific targeting to the organelles, allowing us to narrow down the search for candidate targeting signals to the CP sequence and the N-terminal part of the RTD. These sequences were analyzed with three computer programs taking plant presequences into account (Predotar, Psort, and TargetP). None of them predicted significant mitochondrial targeting of the CP. In contrast, all three programs predicted the N-terminal part of the RTD, i.e., amino acids 189 to 423 of P75, to be targeted to mitochondria, with scores ranging from 0.57 to 0.89. A detailed analysis subsequently revealed that the first 57 amino acids of the RTD, i.e., amino acids 190 to 246 of P75, were entirely responsible for the mitochondrial targeting prediction. This sequence will be referred to as the MTS (for "mitochondrial targeting sequence").

Subcellular targeting of P75 deletion mutants in protoplasts. The putative in vivo targeting properties of the computer-predicted MTS were analyzed with *N. tabacum* BY2 protoplasts and GFP fusions. The expression of GFP fusion proteins in the context of a virus infection was obtained by using a BNYVV RNA-3-derived replicon (16) retaining the noncoding sequences necessary for its recognition by the viral RNA polymerase (29). Such constructs were expressed either in the presence of wild-type BNYVV RNA-1 and -2, to synthesize all RNA-2-encoded proteins as well as the polypeptide encoded by the replicon, or in the presence of RNA-1 alone, which allowed the synthesis of only the replicon-encoded polypeptide.

When GFP alone was expressed in BY2 protoplasts from construct pRep-GFP (Fig. 1D), diffuse fluorescence was present in the cytosol (Fig. 2G to I) and the nucleus (not shown). It was shown previously (15) that GFP fused to amino acids 1 to 423 of P75 (construct pB2-RT-GFP1) (Fig. 1B) is targeted to the mitochondrial periphery, forming well-defined fluorescent rings (Fig. 2A to C). In contrast, GFP fused to a mutant P75 in which amino acids 217 to 250 were deleted (construct pB2-RT-Δ50-GFP2) (Fig. 1C) showed no mitochondrial localization (Fig. 2D to F), and the observed distribution of diffuse fluorescence in the cytosol and nucleus was similar to that obtained with GFP alone. This implied that mitochondrial targeting was lost upon elimination of the C-terminal half of the MTS domain. As a reverse experiment, GFP was fused to the full computer-predicted MTS domain (amino acids 190 to 246 of P75) complemented with an N-terminal methionine replacing the stop codon of ORF1 (construct pRep-MTS-GFP) (Fig. 1D). The expression of this fusion protein in plant protoplasts produced diffuse fluorescence in the cytosol and nucleus, supplemented by rings of more pronounced fluorescence around organelles identified as mitochondria by staining with MitoTracker (Fig. 2J to L). However, the fluorescent rings around the mitochondria were much less intense than those observed with the pB2-RT-GFP1 construct (Fig. 2A to C). Such a mixed distribution between mitochondria and the cytosol indicated that mitochondrial targeting of the MTS-GFP fusion was taking place but that the association with the organelles was of relatively low stability. Thus, our findings suggest that the MTS domain can direct the GFP to mitochondria but is unable to efficiently anchor the fluorescent marker to the organelles. Extending the domain fused to the GFP to amino acid 272 of P75 (construct pRep-MTS-IS-GFP) (Fig. 1D) did not alter the behavior of the fusion protein, implying that amino acids 247 to 272 (which we shall refer to as the "intermediate sequence" [IS]) do not contain information permitting a stable mitochondrial association.

Identification of a candidate sequence for mitochondrial anchoring. The above results suggested that the properties of the MTS domain were restricted to the recognition of mitochondria and that a stable association with the organelles required anchoring to the mitochondrial outer membrane mediated by further sequences in the proximal part of the P75 RTD or in the CP. Three transmembrane domain prediction programs (Argos, TMPRED, and von Heijne) were used to explore the CP and RTD sequences. All three programs predicted that amino acids 276 to 300 of P75 should form a major transmembrane domain. This hydrophobic segment was previously proposed to be a transmembrane domain by Adams et al. (1). A similar hydrophobic segment is conserved in the readthrough proteins of other viruses transmitted by soil fungi

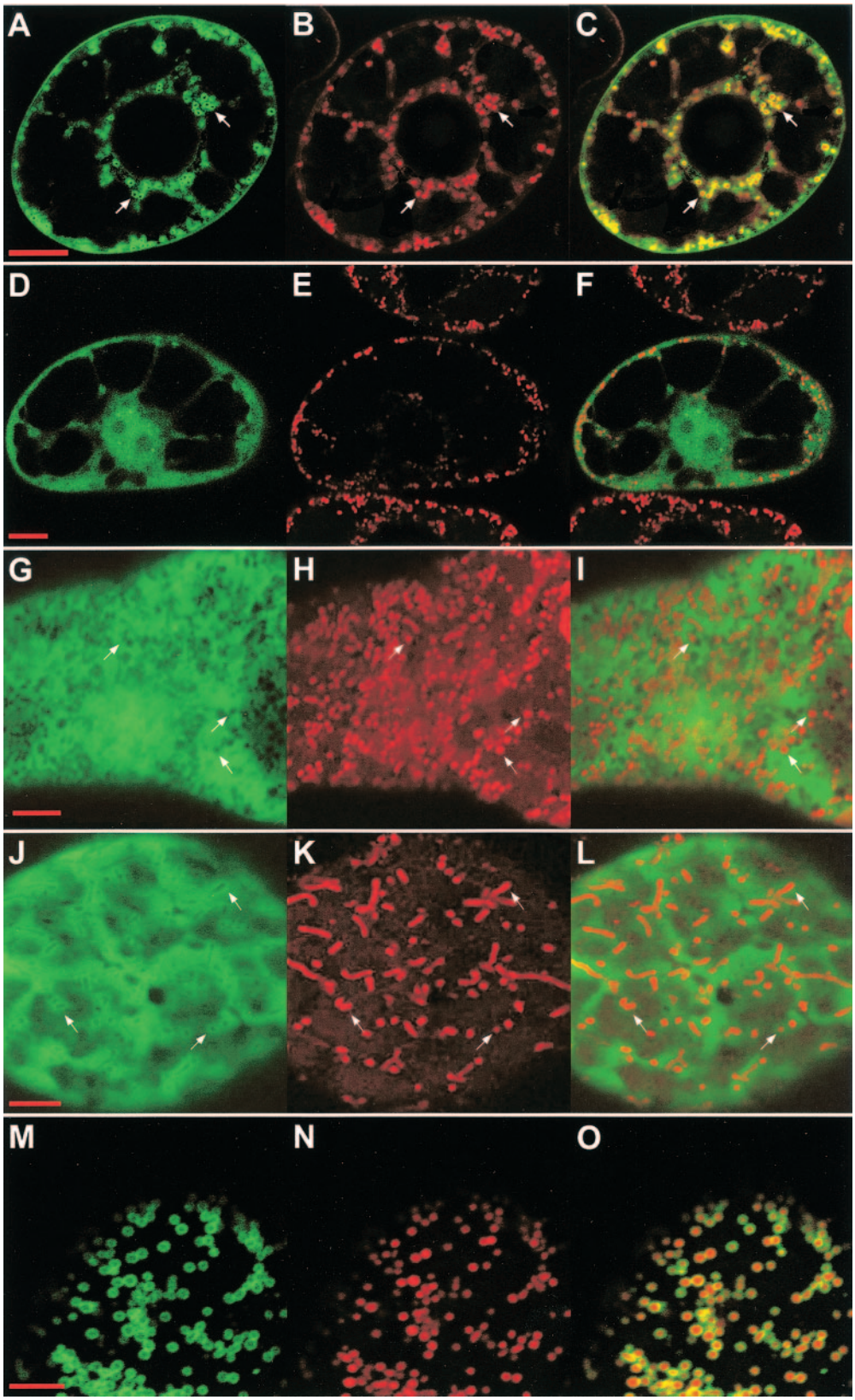

FIG. 2. Expression of GFP-fused P75 deletion mutants in plant protoplasts. *N. tabacum* BY2 protoplasts were infected with BNYVV RNA-1 and the in vitro transcripts derived from constructs pB2-RT-GFP1 (panels A to C), pB2-RT-Δ50-GFP2 (panels D to F), pRep-GFP (panels G to I), pRep-MTS-GFP (panels J to L), and pRep-MTS-IS-TM1-GFP (panels M to O). Expression was analyzed by confocal microscopy 48 h after infection. Panels A, D, G, J, and M display the green fluorescence of the GFP; panels B, E, H, K, and N display for the same cells the red fluorescence of the mitochondrion-specific dye MitoTracker; and panels C, F, I, L, and O display merged images. Arrows point to areas which clearly illustrate the localization of the fusion proteins as discussed in the text. Bars, 10 μm for A to F and 5 μm for G to O.

of the genus *Polymyxa*, such as *Beet soil-borne mosaic virus* and *Soil-borne wheat mosaic virus*, or of the genus *Spongospora*, such as *Potato mop-top virus* (1). Amino acids 273 to 303 of P75 will be referred to as TM1 (for "transmembrane domain 1") in accordance with the work of Adams et al. (1).

Stable association of GFP with mitochondria driven by individual domains of P75 in protoplasts. To assess the in vivo properties of the computer-predicted TM1, further GFP fusions were expressed in *N. tabacum* BY2 protoplasts. GFP was first fused to amino acids 190 to 303 of P75, spanning the MTS and TM1 sequences (construct pRep-MTS-IS-TM1-GFP) (Fig. 1D). Expression of this fusion protein in plant protoplasts yielded abundant and intense GFP fluorescent rings around mitochondria (Fig. 2M to O), as identified upon MitoTracker staining, and no diffuse GFP fluorescence in the cytosol. Essentially all mitochondria throughout the cell were targeted, demonstrating that the combination of the MTS and TM1 sequences is sufficient to promote efficient targeting and a stable association of the GFP with the organelles. The same results were obtained 24 or 48 h after infection. At both time points, mitochondria remained intact and were entirely surrounded by the fluorescent fusion protein. The sequence fused to the GFP was then restricted to amino acids 273 to 303 of P75 (pRep-TM1-GFP) (Fig. 1D), eliminating the MTS and retaining only TM1. In that case, the fluorescence of the fusion protein expressed in BY2 protoplasts was stably associated with multiple cellular membrane systems, including the endoplasmic reticulum, the vacuolar membrane, and the nuclear envelope (Fig. 3A to F and data not shown). The TM1 sequence of P75 thus can mediate a stable membrane association of the GFP, but with no target specificity. Starting the domain fused to the GFP at amino acid 247 of P75 (construct pRep-IS-TM1-GFP) (Fig. 1D), i.e., immediately after the MTS, still led to nonspecific membrane localization of the fluorescence (not shown), implying in turn that the IS region between MTS and TM1 has no specific targeting properties.

To confirm that the subcellular localizations observed in a viral context were intrinsic properties of the GFP fusions and were not mediated by other viral proteins, the MTS and TM1 constructs were also transiently expressed under the control of the *Cauliflower mosaic virus* 35S promoter. For that purpose, BY2 protoplasts were transformed with the pΩ-GFP, pΩ-MTS-IS-TM1-GFP, and pΩ-IS-TM1-GFP plasmids (Fig. 1E). In all cases, the transient expression experiments led to the same observations and conclusions as those obtained with virus-mediated expression experiments (not shown).

At this stage, the results suggested that the MTS and TM1 domains contain all the information necessary to specifically target and anchor P75 to the mitochondrial membranes in plant cells. Furthermore, the observed images indicated that P75 does not possess information allowing the import of GFP-tagged proteins into mitochondria, because fluorescence always accumulated around the organelles and never colocalized with the MitoTracker-stained mitochondrial matrix. However, this model did not explain why the mutant P75 in which the C-terminal half of the MTS was deleted (construct pB2-RT-Δ50-GFP) (Fig. 1C) not only displayed no mitochondrial targeting but was uniformly present in the cytosol and the nucleus (Fig. 2D to F). Since the TM1 region was fully intact in this fusion protein, it should have promoted the same nonspecific association with all cellular membrane systems as that obtained with the TM1-GFP fusion (Fig. 3A to F). This observation led to the possibility that the conformation of the RT-Δ50-GFP protein alters its domain accessibility. To further test such a possibility, we analyzed the membrane integration topology of P75 using isolated plant mitochondria.

In vitro anchoring of the complete P75 protein to the outer membranes of isolated plant mitochondria. In the previous assays, we investigated the properties of individual domains associated with GFP. To verify the actual membrane integration topology of the complete viral polypeptide, the P75 protein was synthesized with a cell-free transcription/translation system in the presence of [^{3}H]leucine and subsequently incubated with isolated *S. tuberosum* mitochondria under standard protein import conditions. [^{3}H]Leucine was preferred over [^{35}S]methionine for labeling because the expected anchoring region including TM1 contained no methionine residue but had several leucine residues. To translate only the full-length P75 protein, the leaky stop codon at the end of the CP sequence was replaced by a UAU tyrosine codon in the pB2-UAU construct (Fig. 1F) used as template (50). To confirm that it does not have a role in the association with mitochondria, CP was also included in the assays. It was translated from construct pB2-TS (TS stands for "triple stop") (Fig. 1F), which contained three successive stop codons at the end of the CP sequence to prevent any readthrough (50).

Upon incubation with isolated plant mitochondria under protein import conditions, P75 indeed associated efficiently with the organelles (Fig. 4A). When mitochondria were treated with proteinase K after import and reisolated, a polypeptide of about 9 kDa was protected by the organelles, confirming the anchoring of the protein to the membranes. The proteinase K protection assay was organelle specific, since in parallel assays the P75 protein showed no intrinsic resistance to proteinase K in the absence of mitochondria. In view of the size of the protected fragment, these assays confirmed that P75 does not undergo conventional import into the mitochondrial matrix. When mitochondria were subjected to alkaline carbonate extraction after import and proteinase K treatment and then separated into pellet and supernatant fractions, the 9-kDa protease-protected polypeptide remained associated with the pellet, as expected for an integral membrane protein. In contrast, similar in vitro import experiments confirmed that CP has no significant mitochondrial targeting properties. In some assays, a small amount of CP bound to isolated mitochondria, but neither anchoring to the membrane nor import into the organelles occurred, as no full or partial protection of the protein against proteinase K was ever observed (Fig. 4A).

Considering that a fragment of only 9 kDa was protected against proteinase K upon anchoring to isolated mitochondria (Fig. 4A), it appears that the actual insertion topology of the complete P75 protein into the mitochondrial membrane is likely to be in the N_{cyto}-C_{cyto} orientation, leaving both the CP sequence and the C-terminal part of the RTD on the cytosolic side. If TM1 alone anchored P75 to the membrane, it would be inserted across the mitochondrial outer membrane in an N_{mito}-C_{cyto} or N_{cyto}-C_{mito} orientation, transferring either the CP sequence or the C-terminal part of the RTD to the intermembrane space. Such a topology would allow the protection of a much larger fragment against proteinase K digestion. On the

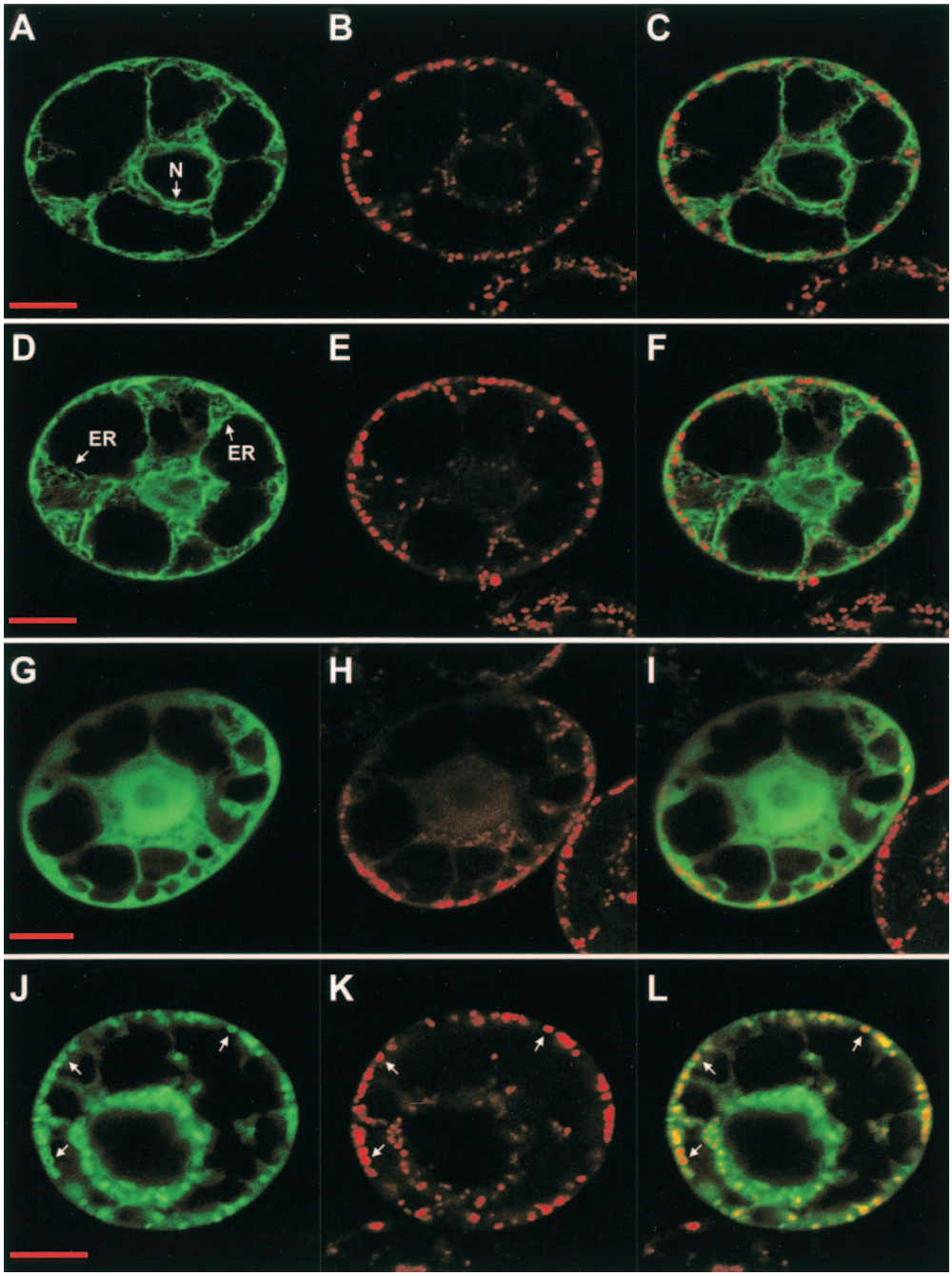

FIG. 3. Expression of GFP fusions with different P75 domains in plant protoplasts. *N. tabacum* BY2 protoplasts were infected with BNYVV RNA-1 and the in vitro transcripts derived from constructs pRep-TM1-GFP (panels A to F), pRep-TM3-TM4-GFP (panels G to I), and pRep-MTS-IS-TM3-TM4-GFP (panels J to L). Expression was analyzed by confocal microscopy 48 h after infection. Panels A, D, G, and J display the green fluorescence of the GFP; panels B, E, H, and K display for the same cells the red fluorescence of the mitochondrion-specific dye MitoTracker; and panels C, F, I, and L display merged images. Arrows point to the nuclear envelope (N) or the endoplasmic reticulum (ER) in panels A to F or to mitochondria in panels J to L. Bars, 10 μm.

other hand, the protected fragment observed seems larger than that expected for an N_{cyto}-C_{cyto} anchoring process in which only TM1 (calculated relative molecular mass of 3.3 kDa) would get embedded in the mitochondrial membrane, especially in view of the fact that the regions upstream of TM1 (CP, MTS, and IS) have no membrane insertion properties. At this stage, we considered an alternative hypothesis, namely, that a second hydrophobic sequence downstream of TM1 is also involved in anchoring, leaving a hydrophilic "loop" protruding inside the intermembrane space between the two transmembrane domains.

Further insights into the functional organization of the P75 protein. A complementary bioinformatic analysis predicted two additional transmembrane domains spanning amino acids

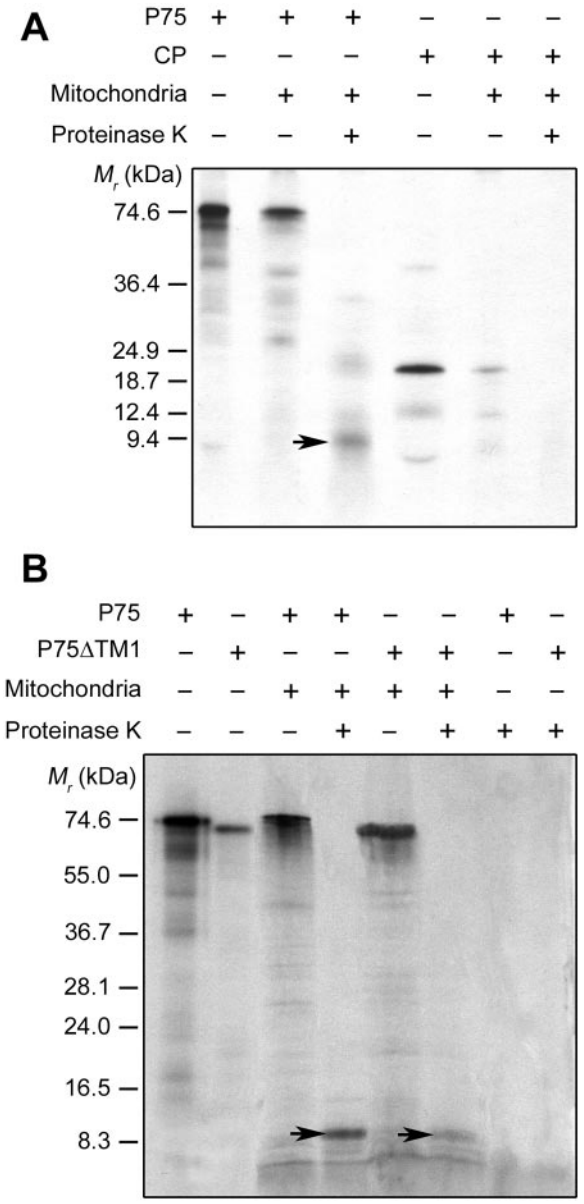

FIG. 4. In vitro anchoring of full-length P75 to isolated plant mitochondria. (A) Labeled P75 and CP were obtained by in vitro transcription/translation of pB2-UAU and pB2-TS, respectively, in the presence of [^{3}H]leucine. (B) Labeled P75 and P75ΔTM1 were obtained by in vitro transcription/translation of pB2-UAU and pB2-UAU-ΔTM1, respectively, in the presence of [^{35}S]methionine. Translation products were incubated with isolated *S. tuberosum* mitochondria under standard import conditions. Mitochondria were subsequently mock treated or treated with proteinase K. Translation products were also treated with proteinase K in the absence of mitochondria. Final samples were analyzed by conventional sodium dodecyl sulfate-polyacrylamide gel electrophoresis and fluorography, along with in vitro-translated or stained marker polypeptides of known molecular masses (left of the panels). The P75-specific 9-kDa polypeptide protected against proteinase K in the mitochondrial fractions is indicated by arrows.

308 to 326 and 373 to 394 of P75. These sequences will be referred to as TM3 and TM4, respectively, to avoid confusion with a more downstream hydrophobic segment (amino acids 555 to 579 of P75) previously proposed as a putative transmembrane domain and named TM2 by Adams et al. (1). The use of [^{3}H]leucine-labeled P75 protein for the above in vitro membrane insertion assays was based on the assumption that the expected anchoring region around TM1 would contain no methionine residue. When the experiments were repeated with [^{35}S]methionine-labeled P75, a similar 9-kDa fragment was protected against proteinase K upon anchoring of the protein to isolated mitochondria (Fig. 4B). The [^{35}S]methionine-labeled P75 protein also showed no intrinsic resistance to proteinase K in the absence of mitochondria (Fig. 4B). This implies that the membrane insertion sequence does in fact contain at least one methionine residue. The first methionine in the RTD is at position 389 of P75 and is included in TM4. The results thus are consistent with an involvement of TM4 in the anchoring of P75 to the mitochondrial outer membrane. As a consequence, whether TM1 is part of the anchored sequence becomes questionable because a proteinase K-resistant fragment spanning TM1 to TM4 would have a larger size (12 kDa) than that experimentally estimated. N_{cyto}-C_{cyto} anchoring of P75 through the transmembrane insertion of TM3 and TM4, with the hydrophilic region between them protruding into the intermembrane space, on the other hand, would be consistent with the in vitro insertion data, as it should yield a protected fragment of the observed size that contains a methionine residue. However, in a gel peptides may migrate differently from expected based on their calculated sizes, which makes it difficult to reliably evaluate such small differences. To gain further information, an [^{35}S]methionine-labeled P75 protein lacking TM1 (P75ΔTM1) was synthesized with a cell-free transcription/translation system using the pB2-UAU-ΔTM1 plasmid (Fig. 1F) as a template. TM1-deprived P75 also associated with isolated *S. tuberosum* mitochondria, and as observed for the full-length protein, a protected polypeptide of about 9 kDa was detected when the import step was followed by proteinase K digestion (Fig. 4B). The fact that the full-length and TM1-deleted P75 proteins yielded membrane-embedded fragments with similar electrophoretic mobilities suggests that TM1 indeed does not substantially contribute to the anchor sequence in the context of the complete protein. Thus, the absence of TM1 did not prevent in vitro anchoring of P75 to the mitochondrial membrane, implying that other sequences can mediate the process. Based on the above considerations, TM3 and TM4 are candidates for such a function.

The properties of the TM3-TM4 domain were tentatively assessed through additional in vivo GFP targeting experiments. GFP was first fused to the TM3-TM4 sequence alone (amino acids 304 to 397 of P75; construct pRep-TM3-TM4-GFP) (Fig. 1D). The expression of such a fusion protein in *N. tabacum* BY2 protoplasts led to diffuse fluorescence in the cytosol and the nucleus (Fig. 3G to I), as observed with GFP alone. Thus, unless its properties are masked in the GFP fusion, the TM3-TM4 domain alone shows no clearly detectable mitochondrial targeting/anchoring capacity in vivo. Also, it does not support an association with multiple cellular membrane systems as does TM1 (Fig. 3A to F). Such an outcome may reflect the fact that TM3 and TM4 are predicted to be weak hydrophobic segments. In contrast, combining both the MTS-IS sequence (amino acids 190 to 272 of P75) and the TM3-TM4 domain (amino acids 304 to 397 of P75) with GFP (construct pRep-MTS-IS-TM3-TM4-GFP) (Fig. 1D) yielded abundant and in-

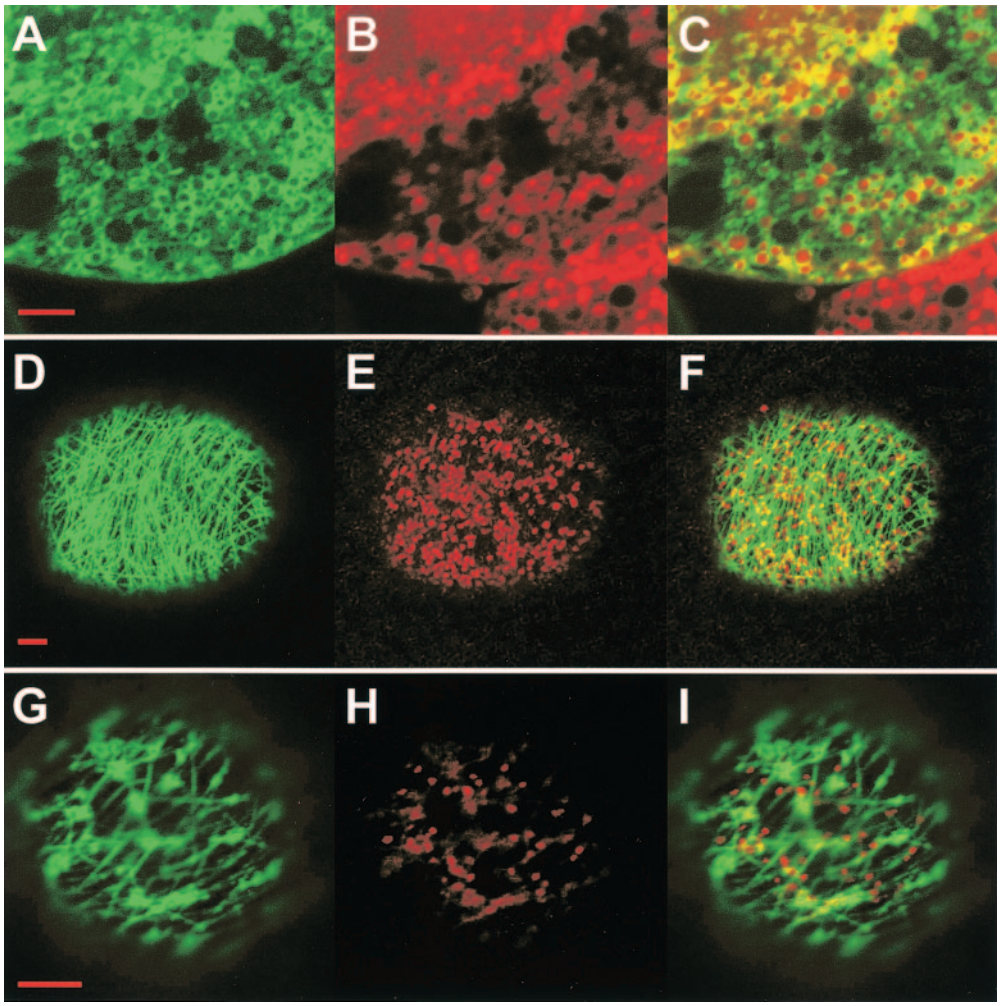

FIG. 5. Expression of a BNYVV RNA-2 GFP fusion construct in plant protoplasts. *N. tabacum* BY2 protoplasts were infected with BNYVV RNA-1 and the in vitro transcript derived from construct pB2-RT-GFP3. The time course of expression and localization was analyzed by confocal microscopy. The images illustrate the three successive localizations of the fluorescence, as rings around mitochondria (panels A to C, taken 24 h after infection), associated with a filamentous network (panels D to F, taken at 30 h), and clustered in the cytosol (panels G to I, taken at 48 h). Panels A, D, and G display the green fluorescence of the GFP; panels B, E, and H display for the same cells the red fluorescence of the mitochondrion-specific dye MitoTracker; and panels C, F, and I display merged images. Bars, 5 μm.

tense fluorescent rings around mitochondria and no diffuse GFP fluorescence in the cytosol (Fig. 3J to L), a pattern similar to that obtained with the MTS-IS-TM1-GFP fusion (Fig. 2M to O). It thus appears that the combination of the MTS and the TM3-TM4 domain is also sufficient to promote efficient targeting and a stable association of the reporter protein with the mitochondria in vivo. These observations are consistent with the above in vitro data and further support the possibility that the TM3-TM4 domain actually anchors the complete P75 protein to the mitochondrial membrane.

In vivo mitochondrial localization of BNYVV particles in plant cells. In the experiments presented above, mitochondrial anchoring of the MTS-IS-TM1-GFP fusion protein expressed in *N. tabacum* BY2 protoplasts from the pRep- or pΩ-based constructs was remarkably efficient. All functional mitochondria were targeted (Fig. 2M to O and data not shown), and the organelle localization was stable throughout the time course used for these studies (i.e., up to 72 h). Similar observations were made with the MTS-IS-TM3-TM4-GFP fusion. Also, the P75 protein anchored to isolated mitochondria was partially resistant to alkaline extraction, which means that it behaved like a stably integrated membrane protein. These results contrasted with the behavior of BNYVV virions, as tested with an additional GFP construct. In this case, we coinfected BY2 protoplasts with BNYVV wild-type RNA-1 and a mutated RNA-2 (synthesized from construct pB2-RT-GFP3) (Fig. 1B) encoding a complete P75 protein carrying the GFP sequence in frame between amino acids 423 and 424. This insertion was located 30 amino acids downstream of TM4 (see above), i.e., outside of the domains putatively involved in mitochondrial targeting and anchoring. The resulting fluorescent viral particles were associated with mitochondria at early times postinfection (starting at 10 to 12 h), with only a fraction of the organelles being targeted (Fig. 5A to C and data not shown). Interestingly, mitochondrial localization of the particles was transient. Eighteen hours after infection, a transition occurred,

with a rapidly growing proportion of the cells having fluorescence that was no longer targeted to mitochondria but was associated with a filamentous network in the cytosol (Fig. 5D to F), suggesting an involvement of the cytoskeleton. Mitochondrial targeting completely disappeared after about 30 h. A further transition from a fluorescent network to clusters of fluorescent bodies in the cytosol (Fig. 5G to I) occurred at later times after infection (starting at 40 h). A similar sequence of events was observed when *C. quinoa* protoplasts were infected (not shown). These observations indicate that, in contrast with GFP fusions containing individual domains of P75, BNYVV virions carrying the complete P75 protein are released from the mitochondria after assembly.

DISCUSSION

The data collected in the present study suggest that BNYVV has developed a mitochondrial targeting strategy based on the minor capsid protein, which is present in only one or a few copies per virion and behaves like an integral protein of the mitochondrial outer membrane. Mitochondrial targeting and import of nucleus-encoded proteins have been extensively characterized for animal, yeast, and plant cells (e.g., see references 25, 32, and 54 and references therein). Most proteins destined for the mitochondrial matrix are synthesized as extended precursors containing a cleavable, positively charged, amino-terminal presequence able to form an amphipathic alpha-helix. Proteins destined for the outer membrane, the intermembrane space, or the inner membrane are generally synthesized as noncleavable mature-sized polypeptides and contain internal information for targeting and sorting. Three mechanisms have been characterized so far for targeting and integration of nucleus-encoded proteins into the mitochondrial outer membrane. Some proteins contain a unique alpha-helix transmembrane domain which functions both as a signal and as an anchor sequence specific for the mitochondrial outer membrane (e.g., see references 2, 28, and 33 and references therein). Insertion leaves domains exposed to the cytosol and to the intermembrane space. This "signal-anchor" mechanism can rely on either an amino-proximal or a carboxy-terminal transmembrane domain (44). The second known targeting mechanism relies on separate import and membrane anchor sequences: an N-terminal or internal matrix-type targeting signal engages transfer through the regular protein import pathway of the outer membrane, i.e., the TOM complex (translocase of the outer membrane), but the transfer is stopped by a hydrophobic domain, which results in membrane anchoring (48). Such a "stop-transfer" mechanism can also apply to proteins containing two transmembrane segments (9). A third class of outer membrane proteins are devoid of uniformly hydrophobic alpha-helix transmembrane domains and are targeted without the aid of a presequence (44). In this case, the targeting and membrane insertion information is contained in structural elements and in the beta-barrel folding of the polypeptide formed by 12 to 14 antiparallel beta-sheets (e.g., see references 8 and 45). Whereas signal-anchored proteins can be directly imported into the outer membrane with the help of the TOM complex, beta-barrel proteins seem to be translocated through the TOM complex to the intermembrane space and subsequently inserted into the outer membrane through the sorting and assembly machinery (SAM complex) (40).

None of the mechanisms described above seems to apply to the BNYVV P75 protein, which has developed an original localization pathway. P75 does not contain a signal-anchor, as the specific recognition of mitochondria and the anchoring to the membrane are mediated by distinct and independent domains. The MTS sequence has specific targeting properties but is unable to stably associate with a membrane. Conversely, the hydrophobic domains involved in P75 membrane anchoring cannot specify organelle targeting, as deletion of the MTS sequence abolishes mitochondrial localization. The stop-transfer mechanism does not apply either because both in vivo and in vitro experiments showed that the BNYVV P75 MTS sequence is unable to promote transfer through the protein import pathway, so there is no transfer to be stopped when a transmembrane domain is reached. Finally, P75 contains a hydrophilic targeting sequence and uniformly hydrophobic stretches for membrane insertion and does not appear to be a beta-barrel-like polypeptide. Thus, BNYVV has developed a pathway involving a targeting sequence able to bring P75 in contact with the mitochondrial membrane with a sufficient affinity to enable subsequent anchoring through hydrophobic domains which have no organelle specificity by themselves. The BNYVV MTS cannot engage import, but considering its scores when analyzed with prediction software, it is likely to have enough similarity with the presequences of authentic mitochondrial proteins to recognize the regular protein import receptors of the TOM complex. Contrasting with the pathway taken by the BNYVV minor coat protein, the viral replicases which have been shown to be mitochondrially targeted (those of *Flock house virus*, *Greasy grouper nervous necrosis virus*, and *Carnation Italian ringspot virus*) seem to have adopted a signal-anchor strategy involving one or two transmembrane domains (20, 34, 55).

An intriguing aspect of the anchoring of P75 to the mitochondrial membrane is the apparent flexibility in the recruitment of the hydrophobic domains ensuring membrane integration. From computer analysis and from the literature (1), TM1 (amino acids 273 to 303 of P75) is the major hydrophobic domain in the N-terminal part of the RTD. Gain-of-function experiments with GFP fusions showed that TM1 is able to cooperate with the MTS to support anchoring of a reporter protein to the mitochondrial membrane. However, the deletion of TM1 from the otherwise complete P75 does not seem to greatly alter anchoring of the viral protein to the outer membranes of isolated mitochondria. It thus appears that different hydrophobic domains can promote membrane anchoring after recognition of the mitochondria by the MTS. Indeed, the two other hydrophobic domains in the proximal part of the RTD, i.e., TM3 (amino acids 308 to 326 of P75) and TM4 (amino acids 373 to 394), are also able to support the MTS-mediated mitochondrial targeting in vivo. From the collected data, it seems plausible that the TM3-TM4 domain actually provides the final membrane-embedded anchor in the complete P75 context. Previous studies have shown that the *Carnation Italian ringspot virus* replicase contains redundant information for mitochondrial targeting (55), so it cannot be excluded that BNYVV P75 similarly possesses redundant information for membrane insertion. However, it seems likely

that the role of the different TM domains in the interaction of P75 with the mitochondria is determined by their accessibility in the overall architecture of the protein and their presentation to the membrane. The same is true for the MTS, especially since it is not located at the N terminus of P75. In this respect, the absence of membrane localization observed when a mutant P75 derived from construct pB2-RT-Δ50-GFP2 (lacking the C-terminal half of the MTS) was expressed in plant cells (Fig. 2D to F) probably means that TM1, although present, was not available for membrane interaction because of the folding of the protein. In the same context, the TM3-TM4 domain, even if not affected, did not have membrane targeting properties in the absence of a complete MTS.

The characterization of the BNYVV protein and subdomains involved in mitochondrial targeting of the virus provides further insight into the infection cycle. Earlier findings showed that expression of the P75 RTD is not required for viral RNA replication and cell-to-cell movement (19, 50). BNYVV particles are associated with mitochondria at a relatively early stage in the infection process, which may be concurrent with virion assembly (15). The effect on virus assembly of short in-frame deletions in the N-terminal part of the RTD of P75 (amino acids 190 to 423) was tested previously (53). Interestingly, deletions in the domains shown in the present work to be involved in mitochondrial targeting and anchoring strongly impaired the encapsidation of the progeny viral RNAs. On the other hand, deletions in the C-terminal half of the P75 RTD, which is dispensable for mitochondrial targeting, did not affect encapsidation (50, 53). It thus seems likely that the association of the P75 protein with mitochondria is required for the efficient assembly of BNYVV particles. Also, there are no assembly-dispensable sequences within the N-terminal part of the P75 RTD, which reinforces the above consideration that the overall conformation of this region determines the topology and efficiency of anchoring to the mitochondrial membrane.

A further question is the potential role of mitochondrial anchoring in BNYVV assembly. A possible response to this question is provided by observations made with *African swine fever virus*-infected cells (49). In this case, virions did not anchor to the organelles but mitochondria migrated to the viral assembly sites, suggesting that mitochondria are recruited to supply energy for virus morphogenetic processes. Similarly, BNYVV particle assembly might be clustered around mitochondria to benefit from the energy provided by the organelles. How viral RNAs and proteins, which are synthesized at different sites, would migrate towards mitochondria to meet in such organelle-anchored virion "factories" is another intriguing question.

In previous experiments, Erhardt et al. (15) coinfected *C. quinoa* leaves or *N. tabacum* protoplasts with BNYVV wild-type RNA-1 and a mutated RNA-2 in which the GFP sequence replaced amino acids 424 to 561 of P75. The GFP sequence either was inserted in frame, so as to allow translation of the downstream C terminus of P75, or was provided with a stop codon, thus restricting the fusion to the N-terminal part of P75 down to amino acid 423. In both cases, the resulting fluorescent viral particles were organized as rings around mitochondria at early times postinfection and later clustered into semi-ordered arrays in the cytosol (15). Whether the particles were released from the mitochondria or whether the virus-loaded mitochondria degenerated could not be determined from these experiments. For the present work, we used a similar approach, but we inserted the GFP gene in frame, without a stop codon, into the complete P75 protein sequence to retain an intact domain from amino acids 424 to 561. Before clustering in the cytosol, the fluorescent virions produced in *N. tabacum* or *C. quinoa* protoplasts infected with this construct appeared to migrate from mitochondria to filamentous structures which we assumed to be part of the cytoskeleton. Such pictures were not observed with the earlier constructs of Erhardt et al., which implies that the putative interaction with the cytoskeleton was mediated by neither the N-terminal nor the C-terminal domain of the P75 RTD but required information present in the region from amino acids 424 to 561. Interestingly, this region contains part of the conserved TM2 transmembrane domain (amino acids 555 to 579 of P75) previously highlighted by Adams et al. (1). They proposed that TM2 would facilitate the movement of virus particles across the fungal membrane during transmission. Our observations identify this hydrophobic domain as a candidate for a role in virion movement inside the plant cell, possibly through an interaction with the cytoskeleton. It thus appears that targeting of the BNYVV P75 protein to mitochondria mediated by the MTS and TM domains located in the N-terminal part of the RTD is but one aspect of a more complex process and that subsequent virion release from mitochondria during the infection cycle involves further signals and factors. Considering the importance of the architecture of P75 for the function of its different domains, as suggested by the present work, it is tempting to speculate that release from the mitochondria might be a consequence, at least in part, of structural changes in P75 following assembly into viral particles.

ACKNOWLEDGMENTS

We thank D. Scheidecker for skillful technical assistance, K. Richards for a critical reading of the manuscript, and P. Hamman and M. Alioua for sequencing of gene constructs.

This work was supported by the Centre National de la Recherche Scientifique (CNRS, UPR2357) and the Université Louis Pasteur (ULP). C.V. was funded by a Ph.D. fellowship from the French Ministère de l'Enseignement Supérieur et de la Recherche. G.V. was funded by a CIFRE fellowship provided by SES Advanta. The microscopy platform used for the present study was cofinanced by the CNRS, the ULP, the Ligue Nationale Contre le Cancer, the Association pour la Recherche contre le Cancer (ARC), and the Région Alsace.

REFERENCES

1. **Adams, M. J., J. F. Antoniw, and J. G. Mullins.** 2001. Plant virus transmission by plasmodiophorid fungi is associated with distinctive transmembrane regions of virus-encoded proteins. Arch. Virol. **146:**1139–1153.
2. **Ahting, U., T. Waizenegger, W. Neupert, and D. Rapaport.** 2005. Signal-anchored proteins follow a unique insertion pathway into the outer membrane of mitochondria. J. Biol. Chem. **280:**48–53.
3. **Beatch, M. D., and T. C. Hobman.** 2000. *Rubella virus* capsid associates with host cell protein p32 and localizes to mitochondria. J. Virol. **74:**5569–5576.
4. **Bleykasten, C., D. Gilmer, H. Guilley, K. E. Richards, and G. Jonard.** 1996. *Beet necrotic yellow vein virus* 42 kDa triple gene block protein binds nucleic acid *in vitro*. J. Gen. Virol. **77:**889–897.
5. **Bouzoubaa, S., L. Quillet, H. Guilley, G. Jonard, and K. Richards.** 1987. Nucleotide sequence of *Beet necrotic yellow vein virus* RNA-1. J. Gen. Virol. **68:**615–626.
6. **Bouzoubaa, S., and D. Scheidecker.** 1990. Infection of protoplasts with *Beet necrotic yellow vein virus* RNA, vol. 1, p. 16–20. *In* R. Koenig (ed.), Proceedings of the First Symposium of the International Working Group on Plant Viruses with Fungal Vectors. Eugen Ulmer Verlag, Stuttgart, Germany.
7. **Buck, K. W.** 1996. Comparison of the replication of positive-stranded RNA viruses of plants and animals. Adv. Virus Res. **47:**159–251.

8. **Casadio, R., I. Jacoboni, A. Messina, and V. De Pinto.** 2002. A 3D model of the voltage-dependent anion channel (VDAC). FEBS Lett. **520:**1–7.
9. **Cohen, I., F. Guillerault, J. Girard, and C. Prip-Buus.** 2001. The N-terminal domain of rat liver carnitine palmitoyltransferase 1 contains an internal mitochondrial import signal and residues essential for folding of its C-terminal catalytic domain. J. Biol. Chem. **276:**5403–5411.
10. **Cserzo, M., E. Wallin, I. Simon, G. von Heijne, and A. Elofsson.** 1997. Prediction of transmembrane alpha-helices in prokaryotic membrane proteins: the dense alignment surface method. Protein Eng. **10:**673–676.
11. **Dunoyer, P., E. Herzog, O. Hemmer, C. Ritzenthaler, and C. Fritsch.** 2001. *Peanut clump virus* RNA-1-encoded P15 regulates viral RNA accumulation but is not abundant at viral RNA replication sites. J. Virol. **75:**1941–1948.
12. **Dunoyer, P., S. Pfeffer, C. Fritsch, O. Hemmer, O. Voinnet, and K. E. Richards.** 2002. Identification, subcellular localization and some properties of a cysteine-rich suppressor of gene silencing encoded by *Peanut clump virus*. Plant J. **29:**555–567.
13. **Dunoyer, P., C. Ritzenthaler, O. Hemmer, P. Michler, and C. Fritsch.** 2002. Intracellular localization of the *Peanut clump virus* replication complex in tobacco BY-2 protoplasts containing green fluorescent protein-labeled endoplasmic reticulum or Golgi apparatus. J. Virol. **76:**865–874.
14. **Emanuelsson, O., H. Nielsen, S. Brunak, and G. von Heijne.** 2000. Predicting subcellular localization of proteins based on their N-terminal amino acid sequence. J. Mol. Biol. **300:**1005–1016.
15. **Erhardt, M., P. Dunoyer, H. Guilley, K. Richards, G. Jonard, and S. Bouzoubaa.** 2001. *Beet necrotic yellow vein virus* particles localize to mitochondria during infection. Virology **286:**256–262.
16. **Erhardt, M., M. Morant, C. Ritzenthaler, C. Stussi-Garaud, H. Guilley, K. Richards, G. Jonard, S. Bouzoubaa, and D. Gilmer.** 2000. P42 movement protein of *Beet necrotic yellow vein virus* is targeted by the movement proteins P13 and P15 to punctate bodies associated with plasmodesmata. Mol. Plant-Microbe Interact. **13:**520–528.
17. **Gallie, D. R., D. E. Sleat, J. W. Watts, P. C. Turner, and T. M. Wilson.** 1987. The 5′-leader sequence of *Tobacco mosaic virus* RNA enhances the expression of foreign gene transcripts *in vitro* and *in vivo*. Nucleic Acids Res. **15:**3257–3273.
18. **Gibbs, J. S., D. Malide, F. Hornung, J. R. Bennink, and J. W. Yewdell.** 2003. The *Influenza A virus* PB1-F2 protein targets the inner mitochondrial membrane via a predicted basic amphipathic helix that disrupts mitochondrial function. J. Virol. **77:**7214–7224.
19. **Gilmer, D., S. Bouzoubaa, A. Hehn, H. Guilley, K. Richards, and G. Jonard.** 1992. Efficient cell-to-cell movement of *Beet necrotic yellow vein virus* requires 3′ proximal genes located on RNA 2. Virology **189:**40–47.
20. **Guo, Y. X., S. W. Chan, and J. Kwang.** 2004. Membrane association of *Greasy grouper nervous necrosis virus* protein A and characterization of its mitochondrial localization targeting signal. J. Virol. **78:**6498–6508.
21. **Haeberle, A., C. Stussi-Garaud, C. Schmitt, J. Garaud, K. Richards, H. Guilley, and G. Jonard.** 1994. Detection by immunogold labelling of P75 readthrough protein near an extremity of *Beet necrotic yellow vein virus* particles. Arch. Virol. **134:**195–203.
22. **Harrison, B. D., and I. M. Roberts.** 1968. Association of *Tobacco rattle virus* with mitochondria. J. Gen. Virol. **3:**121–124.
23. **Harrison, B. D., Z. Stefanac, and I. M. Roberts.** 1970. Role of mitochondria in the formation of X-bodies in cells of *Nicotiana clevelandii* infected by *Tobacco rattle virus*. J. Gen. Virol. **6:**127–140.
24. **Hehn, A., S. Bouzoubaa, N. Bate, D. Twell, J. Marbach, K. Richards, H. Guilley, and G. Jonard.** 1995. The small cysteine-rich protein P14 of *Beet necrotic yellow vein virus* regulates accumulation of RNA 2 in *cis* and coat protein in *trans*. Virology **210:**73–81.
25. **Herrmann, J. M., and W. Neupert.** 2000. Protein transport into mitochondria. Curr. Opin. Microbiol. **3:**210–214.
26. **Herzog, E., O. Hemmer, S. Hauser, G. Meyer, S. Bouzoubaa, and C. Fritsch.** 1998. Identification of genes involved in replication and movement of *Peanut clump virus*. Virology **248:**312–322.
27. **Hofmann, K., and W. Stoffel.** 1992. PROFILEGRAPH: an interactive graphical tool for protein sequence analysis. Comput. Appl. Biosci. **8:**331–337.
28. **Horie, C., H. Suzuki, M. Sakaguchi, and K. Mihara.** 2003. Targeting and assembly of mitochondrial tail-anchored protein Tom5 to the TOM complex depend on a signal distinct from that of tail-anchored proteins dispersed in the membrane. J. Biol. Chem. **278:**41462–41471.
29. **Jupin, I., K. Richards, G. Jonard, H. Guilley, and C. W. Pleij.** 1990. Mapping sequences required for productive replication of *Beet necrotic yellow vein virus* RNA 3. Virology **178:**273–280.
30. **Koulintchenko, M., Y. Konstantinov, and A. Dietrich.** 2003. Plant mitochondria actively import DNA *via* the permeability transition pore complex. EMBO J. **22:**1245–1254.
31. **Laemmli, U. K.** 1970. Cleavage of structural proteins during the assembly of the head of bacteriophage T4. Nature **227:**680–685.
32. **Macasev, D., E. Newbigin, J. Whelan, and T. Lithgow.** 2000. How do plant mitochondria avoid importing chloroplast proteins? Components of the import apparatus Tom20 and Tom22 from *Arabidopsis* differ from their fungal counterparts. Plant Physiol. **123:**811–816.
33. **Mihara, K.** 2000. Targeting and insertion of nuclear-encoded preproteins into the mitochondrial outer membrane. Bioessays **22:**364–371.
34. **Miller, D. J., and P. Ahlquist.** 2002. *Flock house virus* RNA polymerase is a transmembrane protein with amino-terminal sequences sufficient for mitochondrial localization and membrane insertion. J. Virol. **76:**9856–9867.
35. **Nagata, T., Y. Nemoto, and S. Hasezawa.** 1992. Tobacco BY2 cell line as the "HeLa" cell in the cell biology of higher plants. Int. Rev. Cytol. **132:**1–30.
36. **Nakai, K., and M. Kanehisa.** 1992. A knowledge base for predicting protein localization sites in eukaryotic cells. Genomics **14:**897–911.
37. **Neuburger, M., E. P. Journet, R. Bligny, J. P. Carde, and R. Douce.** 1982. Purification of plant mitochondria by isopycnic centrifugation in density gradients of Percoll. Arch. Biochem. Biophys. **217:**312–323.
38. **Niesbach-Klosgen, U., H. Guilley, G. Jonard, and K. Richards.** 1990. Immunodetection *in vivo* of *Beet necrotic yellow vein virus*-encoded proteins. Virology **178:**52–61.
39. **Persson, B., and P. Argos.** 1996. Topology prediction of membrane proteins. Protein Sci. **5:**363–371.
40. **Pfanner, N., N. Wiedemann, C. Meisinger, and T. Lithgow.** 2004. Assembling the mitochondrial outer membrane. Nat. Struct. Mol. Biol. **11:**1044–1048.
41. **Prod'homme, D., A. Jakubiec, V. Tournier, G. Drugeon, and I. Jupin.** 2003. Targeting of the *Turnip yellow mosaic virus* 66K replication protein to the chloroplast envelope is mediated by the 140K protein. J. Virol. **77:**9124–9135.
42. **Putz, C.** 1977. Composition and structure of *Beet necrotic yellow vein virus*. J. Gen. Virol. **35:**397–401.
43. **Quillet, L., H. Guilley, G. Jonard, and K. Richards.** 1989. *In vitro* synthesis of biologically active *Beet necrotic yellow vein virus* RNA. Virology **172:**293–301.
44. **Rapaport, D.** 2003. Finding the right organelle. Targeting signals in mitochondrial outer-membrane proteins. EMBO Rep. **4:**948–952.
45. **Rapaport, D., and W. Neupert.** 1999. Biogenesis of Tom40, core component of the TOM complex of mitochondria. J. Cell Biol. **146:**321–331.
46. **Reichel, C., J. Mathur, P. Eckes, K. Langenkemper, C. Koncz, J. Schell, B. Reiss, and C. Maas.** 1996. Enhanced green fluorescence by the expression of an *Aequorea victoria* green fluorescent protein mutant in mono- and dicotyledonous plant cells. Proc. Natl. Acad. Sci. USA **93:**5888–5893.
47. **Richards, K., G. Jonard, H. Guilley, V. Ziegler, and C. Putz.** 1985. *In vitro* translation of *Beet necrotic yellow vein virus* RNA and studies of sequence homology among the RNA species using cloned cDNA probes. J. Gen. Virol. **66:**345–350.
48. **Rodriguez-Cousino, N., F. E. Nargang, R. Baardman, W. Neupert, R. Lill, and D. A. Court.** 1998. An import signal in the cytosolic domain of the *Neurospora* mitochondrial outer membrane protein TOM22. J. Biol. Chem. **273:**11527–11532.
49. **Rojo, G., M. Chamorro, M. L. Salas, E. Vinuela, J. M. Cuezva, and J. Salas.** 1998. Migration of mitochondria to viral assembly sites in *African swine fever virus*-infected cells. J. Virol. **72:**7583–7588.
50. **Schmitt, C., E. Balmori, G. Jonard, K. Richards, and H. Guilley.** 1992. *In vitro* mutagenesis of biologically active transcripts of *Beet necrotic yellow vein virus* RNA-2: evidence that a domain of the 75 kDa readthrough protein is important for efficient virus assembly. Proc. Natl. Acad. Sci. USA **89:**5715–5719.
51. **Schwer, B., S. Ren, T. Pietschmann, J. Kartenbeck, K. Kaehlcke, R. Bartenschlager, T. S. Yen, and M. Ott.** 2004. Targeting of *Hepatitis C virus* core protein to mitochondria through a novel C-terminal localization motif. J. Virol. **78:**7958–7968.
52. **Tamada, T., and H. Abe.** 1989. Evidence that the *Beet necrotic yellow vein virus* RNA-4 is essential for efficient transmission by the fungus *Polymyxa betae*. J. Gen. Virol. **70:**3391–3398.
53. **Tamada, T., C. Schmitt, M. Saito, H. Guilley, K. Richards, and G. Jonard.** 1996. High resolution analysis of the readthrough domain of *Beet necrotic yellow vein virus* readthrough protein: a KTER motif is important for efficient transmission of the virus by *Polymyxa betae*. J. Gen. Virol. **77:**1359–1367.
54. **Truscott, K. N., K. Brandner, and N. Pfanner.** 2003. Mechanisms of protein import into mitochondria. Curr. Biol. **13:**R326–R337.
55. **Weber-Lotfi, F., A. Dietrich, M. Russo, and L. Rubino.** 2002. Mitochondrial targeting and membrane anchoring of a viral replicase in plant and yeast cells. J. Virol. **76:**10485–10496.
56. **Wischmann, C., and W. Schuster.** 1995. Transfer of *rps10* from the mitochondrion to the nucleus in *Arabidopsis thaliana*: evidence for RNA-mediated transfer and exon shuffling at the integration site. FEBS Lett. **374:**152–156.